

Article pubs.acs.org/JACS

Linear and Radial Conjugation in Extended π -Electron Systems

Garvin M. Peters, Girishma Grover, Ruth L. Maust, Curtis E. Colwell, Haley Bates, William A. Edgell, Ramesh Jasti,* Miklos Kertesz,* and John D. Tovar*



Cite This: https://dx.doi.org/10.1021/jacs.9b10785



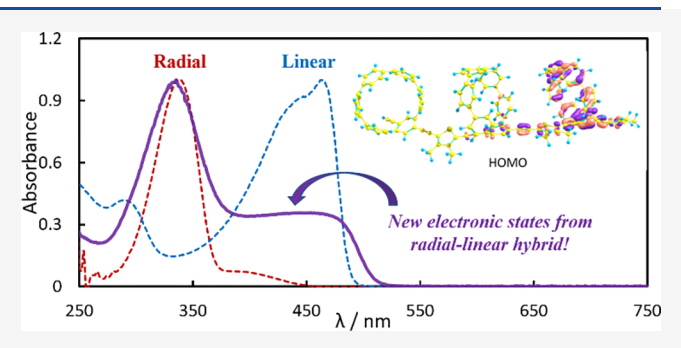
ACCESS

Metrics & More

Article Recommendations

Supporting Information

ABSTRACT: We describe the synthesis and electronic properties of new π -conjugated small molecules and polymers that combine the linear intramolecular conjugation pathways commonly associated with organic electronic materials with the emerging properties of radial conjugation found in cycloparaphenylenes (CPPs) and other curved π -surfaces. Using arylene ethynylenes as prototypical linear segments and [6]/[8]CPP as the radial segments, we demonstrate the formation of new electronic states that are not simply additive responses from the individual components. Quantum chemical calculations of model oligomeric structures reveal these electronic processes to arise from the hybrid



nature of wave function delocalization over the linear and radial contributors in the photophysically relevant electronic states.

INTRODUCTION

Molecules with radial π -conjugation as opposed to the more standard manifestations of linear π -conjugation have fascinated chemists for decades. 1-3 Several isolated examples appeared during this time, including phenylene ethynylene macrocycles⁴ and picotubes,⁵ but the associated synthetic approaches entailed low-yielding multistep routes. In 2008,6 Jasti and Bertozzi demonstrated an efficient chemical synthesis of one class of radially conjugated macrocycles, the cycloparaphenylenes (CPPs), an achievement that catalyzed renewed interest in the area of radial π -conjugation. Alternative synthetic methods were developed (such as those pioneered by Itami and Yamago⁸), and new arylene units were incorporated into the belt-like structures. ^{9–12} The study of more general principles about strain-assisted reactivity 13 and supramolecular interactions 14 was enabled by the size-selective availability of CPPs ranging from 5 to 18 arylene units. CPPs and related curved aromatic molecules can be thought of as diametral segments of (n,n) armchair carbon nanotubes. Indeed, these structures serve as attractive precursors to extended carbon nanotube segments: latently reactive π -conjugated functionality can be incorporated on the CPP "edges" for potential chemistry to zip up a torsionally dynamic precursor into a rigid nanotube segment. 15,16 These and many other studies demonstrate that atomic control over [n]CPP structure allows for new architectures and reactivities beyond models for graphene-like derivatives.

Despite all of these advances, the use of CPP radial conjugation has not been utilized in the design of π -conjugated polymeric materials, where the nature of the π -electron circuits plays a critical role in defining the resulting electronic properties. Given that radical ions created within CPPs are

known to delocalize partially or entirely around the cyclic frameworks depending on the molecular size, 17-20 we felt this would be an attractive motif to extend delocalization in conjugated polymer systems whereby excitons or charge carriers would freely migrate along the linear π -conjugated backbone as well as radially through the CPP structure. This combination of radial and linear conjugation could open up new possibilities for interpolymer energy migration or even supramolecular sensing schemes that blend the molecular selectivity expected for CPPs with the sensitivity enhancements known for π -conjugated electronic polymers. In this report, we describe the synthesis of polymerizable CPP monomers and their subsequent polymerization into conjugated polymers. We present computational studies to better understand the observed electronic processes and to provide insight for future designs. The electronic properties of these materials reveal unusual modes of delocalization not afforded by either the curved or linear π -conjugation pathways in isolation and offers a new vista for conjugated polymer electronics.

RESULTS AND DISCUSSION

Design. To extend linear π -extension onto the CPP cores, [6]- and [8]CPP macrocycles were synthesized with alkynes positioned para to each other on one phenylene unit, thus establishing nascent linear conjugation pathways. These π -

Received: October 7, 2019 Published: January 14, 2020



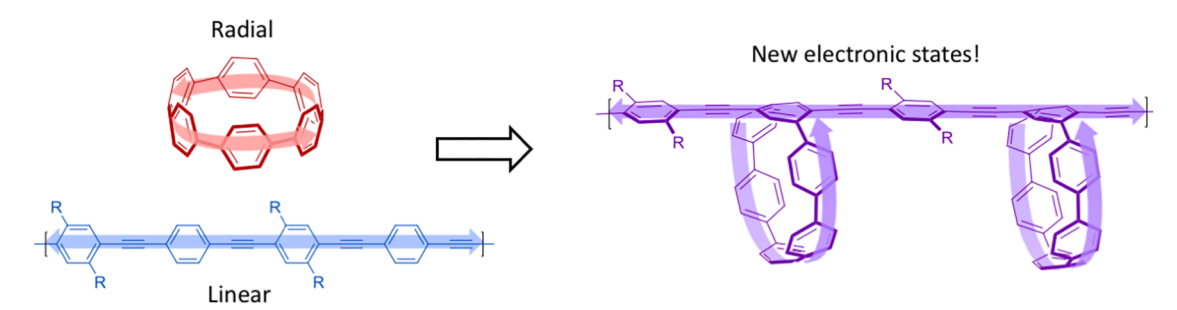


Figure 1. Linear and curved delocalization pathways (left) can be conceptually merged into new π -electron materials (right).

extending units were necessarily ortho-substituted to the macrocycle ring connections, and this tetra-substituted phenylene unit effectively acts as a central hub for both cyclic/radial conjugation around the curved macrocycle and linear conjugation through the conjugated alkyne substitutions (Figure 1, right). One would expect electronic delocalization to be distributed over both the linear π -system of the conjugated backbone and that of the orthogonal curved CPP unit. Thus, intermolecular interactions could be facilitated not only by the planar, rod-like π -surfaces of the main chain but also by the convex and concave surfaces of the off-chain CPPs. We initially targeted a series of conjugated materials that showed intimate mixing of CPP and linear polymer electronic states. To help understand these properties, we also prepared a series of well-defined polymer and small molecule model systems for spectroscopic and computational comparisons.

Linear π -extension of the CPP cores was first realized in the simplest cases through diarylation, where either phenylene or thiophene rings were incorporated to produce small molecules [n]-Ph and [n]-Th (Chart 1a). Model systems T-Ph and T-Th are based on terphenyl, in which the central benzene is

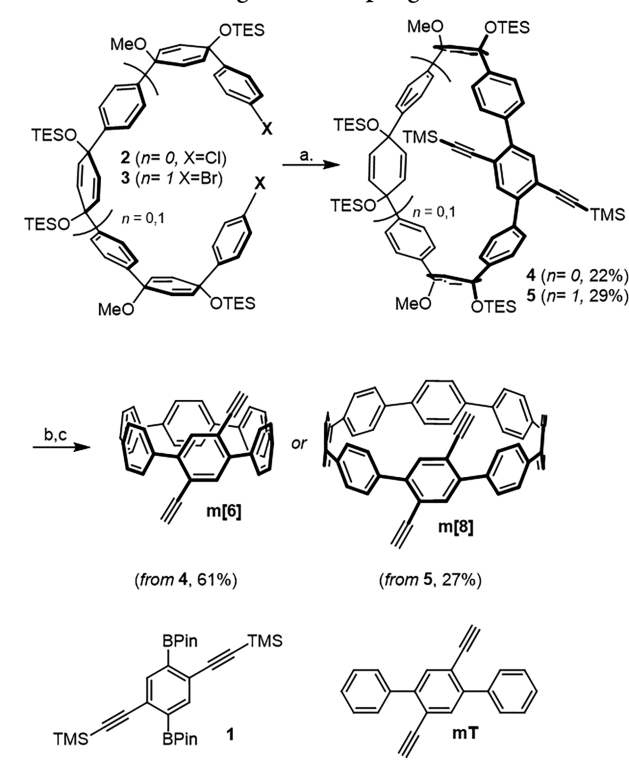
Chart 1. Structures of Small Molecule and Polymeric CPP Systems with Linear π -Extension along with Model Terphenyl Variants (R = 2-Ethylhexyl, R' = Octyl, Ph = Phenyl, Th = Thiophen-2-yl)

analogous to the tetra-substituted ring featured in these CPPs and was also synthesized to allow for comparisons between curved orthogonal π -systems and those that are linear. This also bears other consequences: whereas the phenylene units within the macrocycle have a small amount of conformational freedom, they are relatively rigid in comparison to the phenylenes present in terphenyl. These small model systems were then extrapolated to the analogous polymer systems (P[n]-Ph and P[n]-Th, Chart 1b), which feature furtherextended linear conjugated backbones but also introduce isomeric variance. For example, one would expect that for the polycondensations reported herein, the pendant macrocycles along the conjugated backbone can orient themselves parallel to each other, zig-zagged, or a combination of the two. These hybrid polymers are compared to model terphenyl polymers (PT-Ph and PT-Th) where the off-chain phenylene units are also free to rotate to avoid steric congestion unlike the constrained CPP phenylene units.

Synthesis. In order to incorporate polymerizable functionality into CPP monomers, we adapted our well-established modular building block approach using cyclohexadiene moieties as masked benzene rings (Scheme 1).²¹ The key tetrasubstituted benzene ring linchpin 1²² was prepared on multigram scale from dibromodiiodobenzene via successive Sonogashira couplings (to install TMS acetylene) and Suzuki-Miyaura borylation (to install pinacolborane). Advanced CPP intermediates 2²³ and 3²⁴ were prepared using known synthetic methods developed previously by Jasti and coworkers involving lithiation-addition steps with high control of diastereoselectivity, followed by protection of the resultant alcohols as methyl or triethylsilyl ethers. In this manner, curved intermediates with varying numbers of phenyl rings or cyclohexadienes as masked phenylenes could be assembled rapidly, allowing formation of macrocycles in the next step. Macrocyclizations of either 2 or 3 with bisboronate 1 were then carried out under dilute Suzuki cross-coupling conditions to yield 4 and 5 in 22 and 29% yield, respectively. Finally, global deprotection of the silyl groups and reductive aromatization using mild tin chloride conditions²⁵ yielded the final dialkyne CPP monomers m[6] and m[8] in modest yields (Scheme 1). A dialkynylated terphenyl model system mT (2',5'-diethynyl-p-terphenyl) was also prepared with relative ease in a route mirroring that of 1. 1,4-Dibromo-2,5diiodobenzene was subjected to double Suzuki cross-coupling to chemoselectively assemble the terphenyl core, whereas Sonogashira coupling of TMS acetylene and subsequent silyl deprotection afforded mT.

With the three monomers m[6], m[8], and mT in hand, further linear backbone π -extension was accomplished through Sonogashira cross-coupling reactions, leading to well-defined

Scheme 1. Synthesis of Dialkynes m[6] and m[8] for Linear π -Extension via Sonogashira Couplings^a



"Reaction conditions: (a) 1, SPhos Pd Gen II, K₃PO₄ (aq), dioxane, 80° C; (b) (n-Bu)₄NF, THF, rt; (c) H₂SnCl₄, THF, rt.

small molecule model systems (Chart 1a) as well as polymers (Chart 1b). The small molecules ([6]-Ph, [6]-Th, [8]-Ph, and [8]-Th) consisted of [6]- and [8]CPP with phenylacetylene and thienylacetylene attachments. The polymers (P[6]-Ph,P[6]-Th, P[8]-Ph, and P[8]-Th) were prepared by copolymerization with the respective dialkyne monomers m[6] and m[8] with the corresponding alkylated arylene dihalides. Terphenyl molecular (T-Ph and T-Th) and polymer (PT-Ph and PT-Th) models were derived from similar couplings with mT. Although these molecular reactions went smoothly, there was a fair amount of insoluble compound obtained from the polymerization reactions. Soxhlet extractions with methanol and acetone were used to remove lower molecular weight impurities, and the chloroform extracts were used for photophysical analyses presented here. The GPC molecular weight data for all polymers are presented in Table 1. Although the GPC data for many of the CPP-containing polymers reflect small oligomers, we noted substantial insolubilities in the concentrated THF solutions needed to introduce the polymers into the mobile phase, so the data of Table 1 only reflect the smaller THF soluble oligomers. This insoluble material was similar in appearance to the soluble polymers reported here and potentially represents higher molecular weight material

that either was simply insoluble or may have been supramolecularly cross-linked during polymerization by way of rotaxanation.

Photophysical Properties. Extension of conjugation in m[6] and m[8] along the alkyne-containing pathway proved to be more than a mere amalgamation of the two orthogonal π -systems (Figure 2 and Figure S21), in line with our design

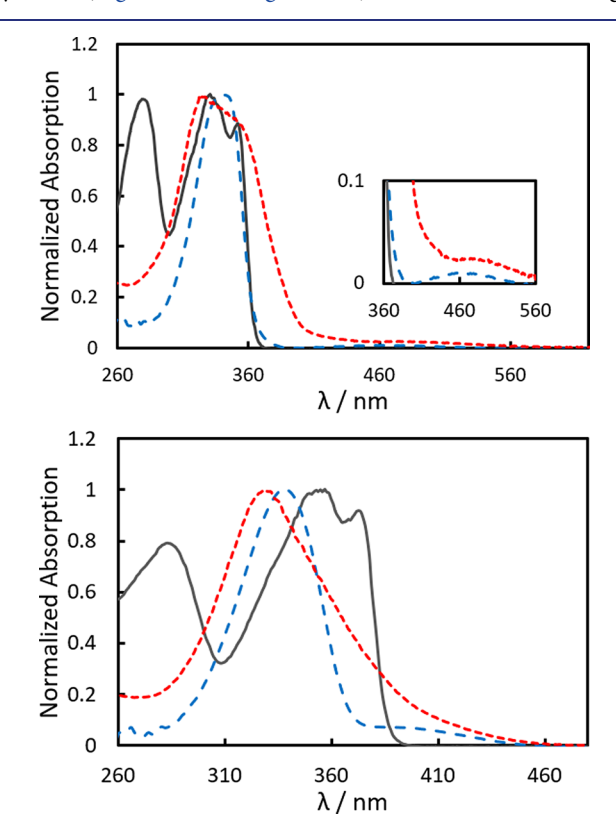


Figure 2. UV—vis spectra recorded in THF for oligomeric [6]-Ph (top) and [8]-Th (bottom) in comparison with the respective CPP and terphenyl model compounds. Top: [6]-Ph (red dotted), T-Ph (gray solid), [6]CPP (blue dashed). The low-energy spectral region is magnified in the inset. Bottom: [8]-Th (red dotted), T-Th (gray solid), [8]CPP (blue dashed).

expectation. In general, [n]CPPs have a characteristic peak absorption at roughly the same energy ($\lambda_{abs} \approx 340$ nm) regardless of size. This corresponds to HOMO-1 and HOMO-2 to LUMO, or HOMO to LUMO+1 or LUMO+2 transitions, as the HOMO-LUMO transition is for the most part forbidden. Smaller CPPs, such as [6]CPP, also feature a very broad low-energy absorption spanning ~400-525 nm (Figure 2, top inset), which is proposed to be a minor contribution from the forbidden HOMO-LUMO transition. Both [6]-Ph and [6]-Th also have this feature (Figure 2, top inset, and Figures S16 and S17), though it is bathochromically shifted and with increased molar absorptivity. The low-energy

Table 1. Distribution of Weight Average (M_w) , Number Average (M_n) Molecular Weight, and Dispersity (\mathfrak{D}) for the Polymer Systems As Determined by Gel Permeation Chromatography in THF along with the Approximate Numbers of Repeat Units

	PT-Ph	PT-Th	P[6]-Ph	P[6]-Th	P[8]-Ph	P[8]-Th
$M_{ m w}$	6877 (~12 repeats)	175548 (~292 repeats)	14765 (~18 repeats)	21599 (~27 repeats)	6333 (~7 repeats)	9061 (~9 repeats)
$M_{\rm n}$	4771 (~8 repeats)	50419 (~84 repeats)	6053 (~8 repeats)	6535 (~8 repeats)	4482 (~5 repeats)	6668 (~7 repeats)
Ð	1.44	3.48	2.44	3.36	1.41	1.36

shoulder seen in [8]CPP (~405 nm)²⁶ is likely buried in the broad low-energy tails of [8]-Ph and [8]-Th. Diarylated monomers [6]-Ph and [6]-Th possessed broadened absorptions that encompass the main CPP absorption, though [6]-Ph has a more pronounced blue shift of the major transition (λ_{max} at 322 nm vs the λ_{max} of 338 nm for [6]-Th). [8]-Ph and [8]-Th similarly demonstrated pronounced blue shifts and broadened spectral footprints compared to parent [8]CPP $(\lambda_{\text{max}} = 321 \text{ nm and } \lambda_{\text{max}} = 329 \text{ nm vs } \lambda_{\text{max}} = 338, \text{ respectively,}$ Figure 2, bottom). The broadness of these absorptions can be attributed to the superimposition of the alkyne-containing linear system with that of the curved CPP macrocycle. The diphenylated CPPs [6]-Ph and [8]-Ph appear to have stronger contributions from the linear segment compared to thienylated species [6]-Th and [8]-Th, where CPP is clearly the major contributor. Spectra recorded in CHCl3 were essentially identical within the useful spectral window to those recorded in THF, indicating that the optical gaps we observe are saturated in both solvents.

To further understand the extent of linear and cyclic conjugation in these well-defined arylene ethynylene/CPP hybrids, their spectral properties were compared to a truncated model whereby the arylene ethynylene is attached to the central ring of a linear p-terphenyl chromophore, yielding T-Ph and T-Th (Chart 1). These models both have a high-energy signature associated with the p-terphenyl core along with structured low-energy absorptions arising from the arylene ethynylene segment (Figure S20) at ~330 and 350 nm (for T-Ph) or at \sim 360 and 375 nm (for T-Th). These structured lowenergy features coincide with those from the CPP itself as well as from the respective [6]-Ph/Th and [8]-Ph/Th small molecule systems, but the lack of fine structure coupled with the spectral broadening in the latter molecules clearly shows that the electronic properties of CPP and the orthogonal arylene ethynylenes are not simply additive but rather that new electronic states are emerging even at this small molecule level. The decreased torsional freedom of the phenylenes when constrained within the CPP core versus the linear terphenyl unit is recognized.

Short π -extensions through addition of benzene or thiophene on the dialkynylated core had subtle but important impacts on the resulting photophysics, and these effects were strongly magnified in the corresponding conjugated polymers. m[6], m[8], and the linear terphenyl model mT were polymerized with either a dialkylated phenyl or thienyl comonomer. As a benchmark, the terphenyl-based polymer with the phenylene ethynylene backbone PT-Ph presented a low-energy absorption at 389 nm (with a pronounced shoulder at ~415 nm) associated with the linearly conjugated backbone, along with higher-energy absorption around 285 nm associated with the terphenyl moiety. P[6]-Ph possessed one major absorption at 348 nm, which correlates with the pendant CPP macrocycle along the polymer backbone (Figure 3), along with a lower-energy broad feature at 438 nm that we assign to the conjugated polymer backbone and the shallow absorption out to 550 nm also found for the parent [6]CPP and [6]-Ph (Figure 2a, inset). Because the shoulder is further red-shifted and broader compared to that of the model polymer's sharp onset of absorption, this is not simply an artifact of any inherent molecular weight differences but suggests new electronic states that are not additive from the [6]CPP and the associated phenylene ethynylene backbone. The analogous thienylene ethynylene P[6]-Th demonstrated similar photo-

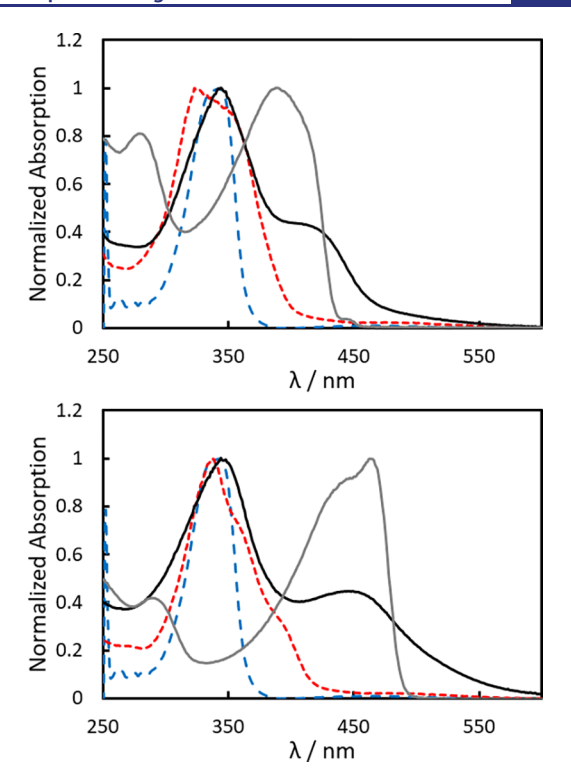


Figure 3. Absorption spectra recorded in THF of [6]CPP polymers with phenylene ethynylene (P[6]-Ph, top) and thienylene ethynylene (P[6]-Th, bottom) linear conjugation linkages, illustrating the impact of gradually extending the orthogonal conjugated system relative to the small molecule models and the polymerized terphenyl analogues. Top: P[6]-Ph (black solid), [6]-Ph (red dotted), PT-Ph (gray solid), [6]CPP (blue dashed). Bottom: P[6]-Th (black solid), [6]-Th (red dotted), PT-Th (gray solid), [6]CPP (blue dashed).

physical responses, showing a broad low-energy ethynylene-based band at 450 nm along with a higher-energy CPP-based band at 350 nm. Here, the low-energy band corresponding to the alkyne-containing conjugated pathway is more coincident with that of the model species PT-Th ($\lambda_{\rm abs}$ at 440 and 465 nm albeit lacking the vibronic structure) and of the shallow tail of the CPP core extending to 550 nm.

As with [6]CPP-containing polymers P[6]-Ph and P[6]-Th, there is little change in the energy of the major [8]CPP-based transition at 335-340 nm upon polymerization of m[8](Figure 4). Both P[8]-Ph and P[8]-Th contain this characteristic signature along with the absorption arising from the conjugated polymer backbone, with variances due to the extent of polymerization. Because the low-energy shoulder (~400-450 nm) associated with [8]CPP molecules extends to a lesser degree into the visible region than [6]CPP, it is more effectively masked by the polymer absorption. However, the much stronger intensities for the low-energy absorptions of the P[8]-Ph and -Th polymers suggest these are not arising solely from CPP-based transitions but rather reflect the dual nature of the cyclic and linear conjugation. This is most pronounced in P[8]-Th, where the broad shoulder extending from \sim 400 to 500 nm is quite distinct from the vibronic features present in the PT-Th model polymer at 440 and 465 nm (Figure 4).

To further probe the electronic processes operative within the hybrid radial—linear π -electron materials, photoluminescence spectra were recorded (Figure 5). [6]CPP by itself is negligibly photoluminescent, and this carried over into [6]-Ph/Th and the corresponding polymers P[6]-Ph/Th. [8]CPP

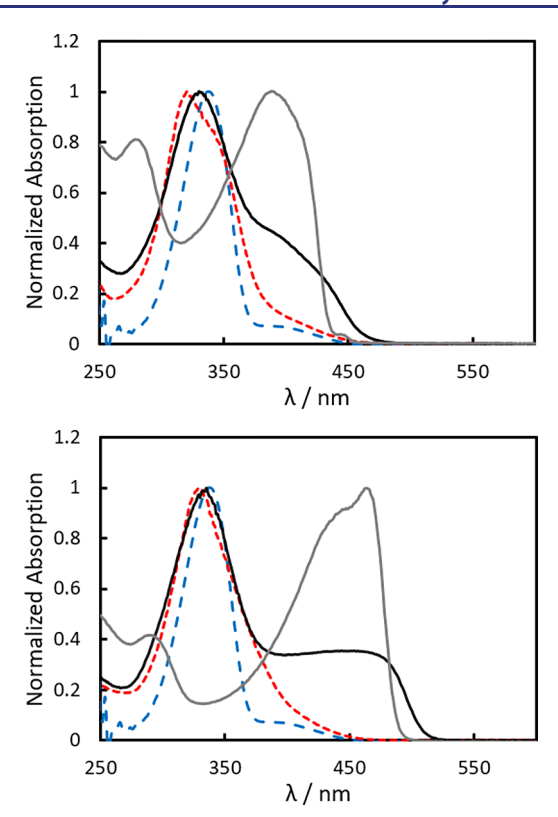


Figure 4. Absorption spectra recorded in THF of [8]CPP polymers with phenylene ethynylene (P[8]-Ph, top) and thienylene ethynylene (P[8]-Th, bottom) linear conjugation linkages, illustrating the impact of gradually extending the orthogonal conjugated system relative to the small molecule models and the polymerized terphenyl analogues. Top: P[8]-Ph (black solid), [8]-Ph (red dotted), PT-Ph (gray solid), [8]CPP (blue dashed). Bottom: P[8]-Th (black solid), [8]-Th (red dotted), PT-Th (gray solid), [8]CPP (blue dashed).

in contrast shows a peak luminescence at 535 nm, and the hybrid materials also show different extents of photoluminescence. The emission profile for the oligomeric and polymeric phenylated [8]CPPs are very similar to this parent CPP emission, although slightly red-shifted (~10-25 nm: Figure 5, top). Notably, the luminescence from the phenylene ethynylene backbone of PT-Ph falls at a much higher energy (430 nm peak emission with a 460 nm vibronic shoulder), which suggests that the CPP moiety is dominating the excited state processes for these structures albeit with some energetic influence from the attached linearly conjugated chains. In the phenylated CPP cases, the substantial Stokes' shifts indicate pronounced excited state planarization/reorganization. In contrast, the emission profile for the thienylated [8]CPP analogues demonstrate much more pronounced differences (Figure 5, bottom). [8]-Th fluorescence almost mirrors that of [8]-Ph, falling at 560 nm, again red-shifted by 25 nm from the [8]CPP core. The corresponding CPP-based thienylene ethynylene polymer P[8]-Th is more drastically blue-shifted and vibronically structured (peaks at 515 and 560 nm) than is [8]-Th but is more red-shifted than is the corresponding terphenyl model PT-Th (with peaks at 485 and 520 nm). Clearly, the excited state electronic structure of P[8]-Th is much more than an additive response from the thienylene ethynylene linear backbone and the CPP radial pendant components.

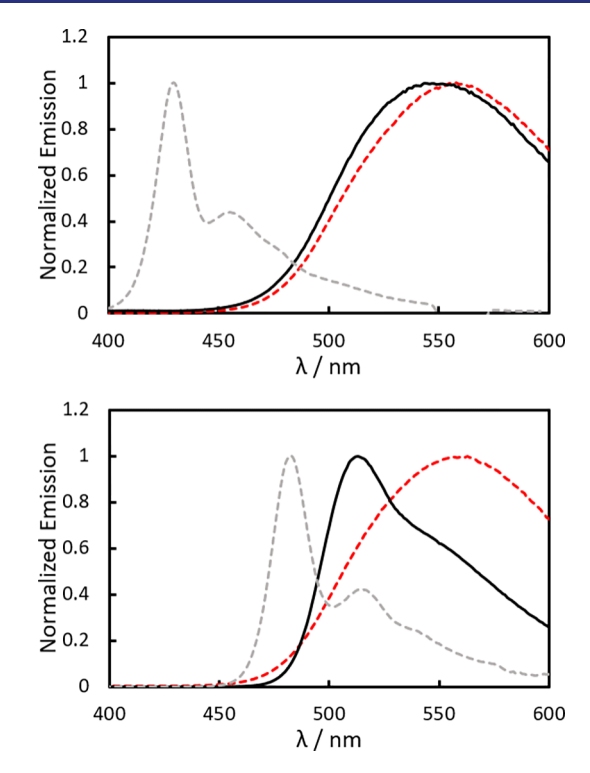


Figure 5. Photoluminescence spectra recorded in THF for [8]CPP-based π -extended small molecules and polymers compared to those of the linear analogues. Top: P[8]-Ph (black solid), [8]-Ph (red dotted), PT-Ph (gray dotted). Bottom: P[8]-Th (black solid), [8]-Th (red dotted), PT-Th (gray dotted).

Computational Studies. All calculations were performed using Gaussian 16.²⁸ All optimizations on small molecules and oligomers were performed using ground state density functional theory calculations with PBE1PBE/6-31G(d).²⁹ Excited state calculations were performed using time-dependent density functional theory. All UV—vis absorption spectra were obtained with broadening of half-width at half-height of 0.2 eV or 1613 cm⁻¹.

We present here our results on oligomeric repeat units of the corresponding polymers. These are named nT-Th/Ph and n[6/8]-Th/Ph, where n refers to the length of the oligomeric repeat unit. For simplifying the calculations, all alkyl groups of the n[6/8]-Th/Ph oligomers were replaced with methyl groups (see details in SI and Figure S1). For example, the trimeric structure of P[6]-Ph with the alkyl groups replaced by methyl groups is named 3[6]-Ph. Before modeling the UV-vis spectra associated with these defined oligomers, we validated our computational approach by using the well-defined molecular structures listed in Chart 1a. Accordingly, the average predicted UV-vis peak positions are 8 nm shifted to the longer wavelengths compared to the respective experiments. The range of this prediction error is between -29 and 24 nm, and the maximum error is 8%. The high reliability of the computations is essential in evaluating the polymer predictions. Furthermore, we assessed the effect of conformational/torsional degrees of freedom along the linear backbones on the UV-vis spectra, an essential element in the discussion of polyaromatic conjugated polymers. As shown in the Supporting Information, variations of the main peak at 450 nm can be as large as 100 nm due to the conformational flexibility around the linear C2 alkyne group. Thus, it is possible that in solution various conformers coexist such that

in some molecules the extended conjugation is disrupted, limiting the effective conjugation length along the main chain as known in other conjugated polymers, as well.³⁰

The polymer UV-vis spectra for all six polymer systems in Table 1 were modeled by a succession of different size oligomers with n = 2, 3, and, in some cases, 4, with details provided in the Supporting Information. The extrapolation to polymers of infinite length was based on a linear regression between $1/\lambda$ of the lowest-energy transition as a function of $1/\lambda$ n.³¹ Accordingly, the predicted long wavelength polymer peak is very substantially red-shifted, as shown in Table S2. For example, for PT-Th, the predicted maximum is at 605 nm, whereas the experimental low-energy peak value is around 440-500 nm. This difference is much larger than expected based on the validation described above. We can see that the corresponding predicted wavelengths for other polymers are still significantly larger (red-shifted), as well, compared to the experiment. Using the $1/\lambda$ versus 1/n linear fit, and substituting the experimental peak value for the polymer, we obtained approximate conjugation lengths that are shown in Table S2. The observed peak wavelength of 440-500 nm of PT-Th corresponds to a chain length of only 1.7-2.7 units, an effective conjugation length corresponding to a dimer or trimer. The fact that the polymer absorption bands are broader than the bands of the monomers then can be attributed to a distribution of different chain lengths and different conformational defects, limiting the range of delocalization to about 2-3units on average. The corresponding conjugation lengths ranges are shown in Table S2.

The experimental molecular weight data indicate diverse ranges of average chain lengths for different polymers ranging from approximately 5 to 292 units (Table 1, which is likely an underestimate based on solubility in the GPC analyte solution and the restricted hydrodynamic radii of the CPP units on the polymer backbones, seeFigure S26). On the other hand, the computed UV-vis spectra data indicate that the effective conjugation length is typically limited to about 1-3 units for these polymers, except for P[6]-Th, which is in the 1–10 unit range (Table S2). For this reason, we argue that conformational defects must be present that reduce the effective conjugation length and limit it to only a few repeat units. With this interpretation, we should not be surprised that the experimentally observed peaks are close to the predicted peaks for the systems such as 2T-Th, 2T-Ph, 2[8]-Th, and 3[6]-Th and not the predicted extrapolated polymer values (Table S2).

The low-energy shoulder observed for the P[n]-Th and -Ph polymers in the UV-vis experiment, especially for P[8]-Th, are indicative of a broad distribution of conjugation lengths. However, the UV-vis spectra alone cannot provide detailed information on such a distribution. It is interesting that the respective UV-vis experimentally observed bands for the model systems without CPP units, PT-Th and PT-Ph are also very broad but appear at a larger relative intensity compared to the higher-energy peaks. The HOMO-LUMO transitions in [n]CPPs are forbidden in the ideal D_{nh} symmetry or nearly forbidden in the real systems that have a lower symmetry. 26,32,33 The respective lowest-energy peaks show up as weak absorption peaks that are increasing in relative intensity as the CPPs are substituted by linearly conjugated side groups. This effect is a proof of the linear-radial conjugation that was postulated at the onset of this study. This linear-radial conjugation effect is completely absent in the terphenyl

derivatives, where this long wavelength tail is missing in the absorption spectrum.

It is important to recognize that the enhanced low-energy shoulder seen in the experimental spectra for the polymers, especially most clearly for P[8]-Th, is not simply an enhanced HOMO-LUMO transition of the [8]CPP part of the polymer. This is most clearly seen in the computed spectrum of 2[8]-Th and 3[8]-Th (Figure S8c,f), where the lowest-energy transition (HOMO to LUMO) with oscillator strength of 1.4 and 2.4, respectively, is localized on the linear conjugated components, unlike the monomer 1[8]-Th (Figure S8a,b), where the major contribution from the radial conjugated component makes the HOMO to LUMO transition with oscillator strength of 0.09 only slightly allowed. These strongly allowed transitions overwhelm the weakly allowed HOMO \rightarrow LUMO transitions of the CPP moieties. The polymers containing [6]CPP are different: here, the CPP and the linear conjugated parts display significant mixing in the HOMO, whereas the LUMO is localized mostly on the linear part (Figure 6).

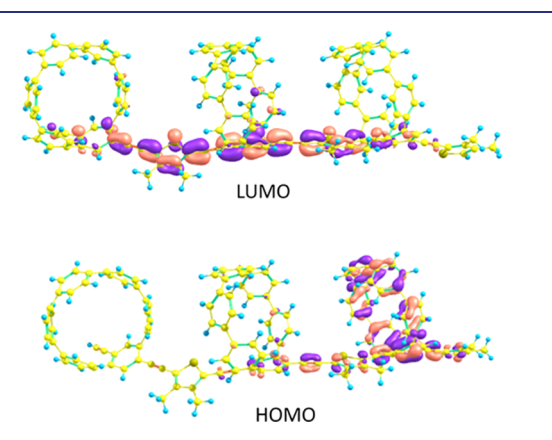


Figure 6. Conjugation in an optimized geometry of **3[6]-Th** in HOMO (bottom) and LUMO (top) orbitals showing the hybrid contributions from both the linear and radial components.

On the other hand, the next two to three higher-energy transitions for all four CPP polymers display various signs of unique behavior not seen in isolated CPPs or in linear conjugated polymers. Although each individual case is different, the following types of such new transitions are seen in the oligomer computations: transitions involving orbitals localized mostly on the CPP part to orbitals localized mostly on the linear part or vice versa. Then some transitions comprise orbitals containing genuine mixing between the linear and radial conjugated components for either one or both orbitals involved in the transition. For example, a strong radial to linear conjugated transition for 3[6]-Ph at 460 nm has a dominant contribution from HOMO-1 to LUMO+1, as illustrated in Figure 7.

The situation for the model systems with terphenyl in place of the CPP components is somewhat different. For both 3T-Th and 3T-Ph, the lowest-energy transition is mostly HOMO → LUMO and includes primarily the main chain. However, this transition does not overlap with the low-energy transition of the terphenyl component as that is not forbidden as opposed to the CPP case. The higher-energy transitions involve orbitals for 3T-Ph that are mostly confined to the main chain. However, in the case of 3T-Th, the higher-energy transitions are similar to those of the CPP-based polymers. The thiophene is linked to the linear chain at the 2,5 positions

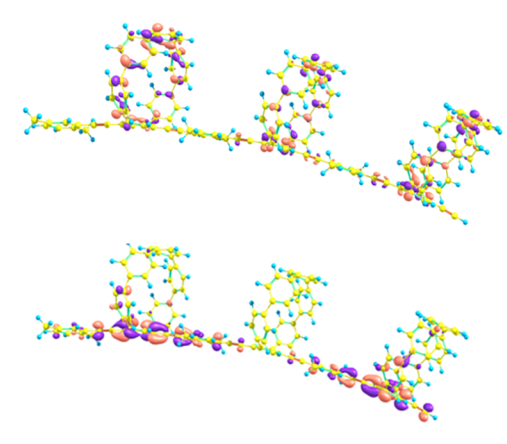


Figure 7. Mixing of linear vs radial conjugation in the computed absorption spectrum of **3[6]-Ph** at 460 nm is evident in the HOMO–1 (top) and LUMO+1 (bottom) surfaces.

in 3T-Th, resulting in a slight bending of the backbone contributing to the disruption of the extended conjugation and thus delocalization on terphenyl. On the other hand, in the case of the phenyl-substituted polymer, the linkage at the 2,5 positions makes the backbone more linear, and thus, the delocalization within the backbone is retained to a larger extent, as illustrated in Figure S22. In the case of 3T-Ph, we observed a behavior similar to that in the CPPs, except the oscillator strength is comparatively smaller.

CONCLUSIONS

Novel CPP syntheses and functionalizations have provided access to a wide range of curved π -conjugated systems possessing intriguing electronic properties. We report latestage modifications of a proven synthetic path toward CPPs to realize dialkyne-functionalized CPP monomers containing 6and 8 phenylene units. Both short and long π -extensions of the radial CPP core were prepared and compared to linear terphenyl model systems to investigate the impact of having a hybrid linear-radial conjugated system. Differences in the absorption and photoluminescence profiles of extended small molecules and polymers attest to the nonadditive combinations of linear and radial π -conjugation, indicating the crafting of new electronic processes in these hybrid materials. Computational modeling suggests that, whereas the effective conjugation lengths of these systems may be limited, there are many accessible electronic states that are well beyond simple combinations of the separate linear and radially oriented conjugation pathways. Our future work will examine new ways to encourage intramolecular and intermolecular electronic delocalization that may take advantage of this merger of linear and radial conjugation.34

ASSOCIATED CONTENT

Supporting Information

The Supporting Information is available free of charge at https://pubs.acs.org/doi/10.1021/jacs.9b10785.

Synthetic and computational procedures, comparisons of calculated and experimental UV—vis absorption energies, computed UV—vis spectra, torsional angle variation studies, orbitals for important energy levels, additional UV—vis experimental spectra, GPC chromatographs, and ¹H and ¹³C NMR spectra (PDF)

AUTHOR INFORMATION

Corresponding Authors

Ramesh Jasti — Department of Chemistry and Biochemistry, Materials Science Institute, and Knight Campus for Accelerating Scientific Impact, University of Oregon, Eugene, Oregon 97403, United States; Occid.org/0000-0002-8606-6339; Email: rjasti@uoregon.edu

Miklos Kertesz — Chemistry Department and Institute of Soft Matter, Georgetown University, Washington, DC 20057, United States; orcid.org/0000-0002-7930-3260; Email: kertesz@georgetown.edu

John D. Tovar — Department of Chemistry and Department of Materials Science and Engineering, Johns Hopkins University, Baltimore, Maryland 21218; orcid.org/0000-0002-9650-2210; Email: tovar@jhu.edu

Authors

Garvin M. Peters – Department of Chemistry, Johns Hopkins University, Baltimore, Maryland 21218

Girishma Grover — Chemistry Department and Institute of Soft Matter, Georgetown University, Washington, DC 20057, United States

Ruth L. Maust – Department of Chemistry and Biochemistry, Materials Science Institute, and Knight Campus for Accelerating Scientific Impact, University of Oregon, Eugene, Oregon 97403, United States

Curtis E. Colwell — Department of Chemistry and Biochemistry, Materials Science Institute, and Knight Campus for Accelerating Scientific Impact, University of Oregon, Eugene, Oregon 97403, United States; Occid.org/0000-0002-4762-1934

Haley Bates – Department of Chemistry, Johns Hopkins University, Baltimore, Maryland 21218

William A. Edgell — Department of Chemistry and Biochemistry, Materials Science Institute, and Knight Campus for Accelerating Scientific Impact, University of Oregon, Eugene, Oregon 97403, United States

Complete contact information is available at: https://pubs.acs.org/10.1021/jacs.9b10785

Notes

The authors declare no competing financial interest.

ACKNOWLEDGMENTS

This material is based upon work supported by the U.S. Department of Energy, Office of Science, Office of Basic Energy Sciences under Award Number DE-SC-0019017. R.M. was supported by the NSF Graduate Research Fellowship (1309047). We thank Mr. Eric Peterson (JHU) for assistance with spectral measurements.

REFERENCES

- (1) Parekh, V. C.; Guha, P. C. Synthesis of p,p-diphenylene disulfide. *J. Indian Chem. Soc.* **1934**, *11*, 95–100.
- (2) Friederich, R.; Nieger, M.; Vögtle, F. Auf dem Weg zu makrocyclischen para-Phenylenen. Chem. Ber. 1993, 126, 1723–1732.
- (3) Scott, L. T. Conjugated Belts and Nanorings with Radially Oriented p Orbitals. *Angew. Chem., Int. Ed.* **2003**, *42*, 4133–4135.
- (4) Kawase, T.; Darabi, H. R.; Oda, M. Cyclic [6]- and [8]Paraphenylacetylenes. *Angew. Chem., Int. Ed. Engl.* **1996**, 35, 2664–2666.
- (5) Kammermeier, S.; Jones, P. G.; Herges, R. Ring-Expanding Metathesis of Tetradehydro-anthracene—Synthesis and Structure of a

- Tubelike, Fully Conjugated Hydrocarbon. *Angew. Chem., Int. Ed. Engl.* **1996**, 35, 2669–2671.
- (6) Jasti, R.; Bhattacharjee, J.; Neaton, J. B.; Bertozzi, C. R. Synthesis, Characterization, and Theory of [9]-, [12]-, and [18]-Cycloparaphenylene: Carbon Nanohoop Structures. *J. Am. Chem. Soc.* **2008**, *130*, 17646–17647.
- (7) Takaba, H.; Omachi, H.; Yamamoto, Y.; Bouffard, J.; Itami, K. Selective Synthesis of [12] Cycloparaphenylene. *Angew. Chem., Int. Ed.* **2009**, *48*, 6112–6116.
- (8) Yamago, S.; Watanabe, Y.; Iwamoto, T. Synthesis of [8]-Cycloparaphenylene from a Square-Shaped Tetranuclear Platinum Complex. *Angew. Chem., Int. Ed.* **2010**, *49*, 757–759.
- (9) Hitosugi, S.; Nakanishi, W.; Yamasaki, T.; Isobe, H. Bottom-up synthesis of finite models of helical (n,m)-single-wall carbon nanotubes. *Nat. Commun.* **2011**, *2*, 492.
- (10) Iwamoto, T.; Kayahara, E.; Yasuda, N.; Suzuki, T.; Yamago, S. Synthesis, Characterization, and Properties of [4]Cyclo-2,7-pyrenylene: Effects of Cyclic Structure on the Electronic Properties of Pyrene Oligomers. *Angew. Chem., Int. Ed.* **2014**, *53*, 6430–6434.
- (11) Matsui, K.; Segawa, Y.; Itami, K. Synthesis and Properties of Cycloparaphenylene-2,5-pyridylidene: A Nitrogen-Containing Carbon Nanoring. *Org. Lett.* **2012**, *14*, 1888–1891.
- (12) Tran-Van, A.-F.; Huxol, E.; Basler, J. M.; Neuburger, M.; Adjizian, J.-J.; Ewels, C. P.; Wegner, H. A. Synthesis of Substituted [8] Cycloparaphenylenes by [2 + 2 + 2] Cycloaddition. *Org. Lett.* **2014**, *16*, 1594–1597.
- (13) Schaub, T. A.; Margraf, J. T.; Zakharov, L.; Reuter, K.; Jasti, R. Strain-Promoted Reactivity of Alkyne-Containing Cycloparaphenylenes. *Angew. Chem., Int. Ed.* **2018**, *57*, 16348–16353.
- (14) Xu, Y.; Wang, B.; Kaur, R.; Minameyer, M. B.; Bothe, M.; Drewello, T.; Guldi, D. M.; von Delius, M. A Supramolecular [10]CPP Junction Enables Efficient Electron Transfer in Modular Porphyrin−[10]CPP⊃Fullerene Complexes. *Angew. Chem., Int. Ed.* **2018**, *57*, 11549−11553.
- (15) Golling, F. E.; Quernheim, M.; Wagner, M.; Nishiuchi, T.; Müllen, K. Concise Synthesis of 3D π-Extended Polyphenylene Cylinders. *Angew. Chem., Int. Ed.* **2014**, *53*, 1525–1528.
- (16) Golder, M. R.; Colwell, C. E.; Wong, B. M.; Zakharov, L. N.; Zhen, J.; Jasti, R. Iterative Reductive Aromatization/Ring-Closing Metathesis Strategy toward the Synthesis of Strained Aromatic Belts. *J. Am. Chem. Soc.* **2016**, 138, 6577–6582.
- (17) Fujitsuka, M.; Tojo, S.; Iwamoto, T.; Kayahara, E.; Yamago, S.; Majima, T. Radical Ions of Cycloparaphenylenes: Size Dependence Contrary to the Neutral Molecules. *J. Phys. Chem. Lett.* **2014**, *5*, 2302–2305.
- (18) Kayahara, E.; Kouyama, T.; Kato, T.; Yamago, S. Synthesis and Characterization of [n]CPP (n = 5, 6, 8, 10, and 12) Radical Cation and Dications: Size-Dependent Absorption, Spin, and Charge Delocalization. *J. Am. Chem. Soc.* **2016**, *138*, 338–344.
- (19) Toriumi, N.; Muranaka, A.; Kayahara, E.; Yamago, S.; Uchiyama, M. In-Plane Aromaticity in Cycloparaphenylene Dications: A Magnetic Circular Dichroism and Theoretical Study. *J. Am. Chem. Soc.* **2015**, *137*, 82–85.
- (20) Talipov, M. R.; Jasti, R.; Rathore, R. A Circle Has No End: Role of Cyclic Topology and Accompanying Structural Reorganization on the Hole Distribution in Cyclic and Linear Poly-p-phenylene Molecular Wires. *J. Am. Chem. Soc.* **2015**, *137*, 14999–15006.
- (21) Darzi, E. R.; Sisto, T. J.; Jasti, R. Selective Syntheses of [7]—[12]Cycloparaphenylenes Using Orthogonal Suzuki—Miyaura Cross-Coupling Reactions. *J. Org. Chem.* **2012**, *77*, 6624—6628.
- (22) Duhović, S.; Dincă, M. Synthesis and Electrical Properties of Covalent Organic Frameworks with Heavy Chalcogens. *Chem. Mater.* **2015**, *27*, 5487–5490.
- (23) Darzi, E. R.; White, B. M.; Loventhal, L. K.; Zakharov, L. N.; Jasti, R. An Operationally Simple and Mild Oxidative Homocoupling of Aryl Boronic Esters To Access Conformationally Constrained Macrocycles. *J. Am. Chem. Soc.* **2017**, *139*, 3106–3114.

- (24) Lovell, T. C.; Colwell, C. E.; Zakharov, L. N.; Jasti, R. Symmetry breaking and the turn-on fluorescence of small, highly strained carbon nanohoops. *Chemical Science* **2019**, *10*, 3786–3790.
- (25) Patel, V. K.; Kayaĥara, E.; Yamago, S. Practical Synthesis of [n] Cycloparaphenylenes (n = 5, 7–12) by H2SnCl4-Mediated Aromatization of 1,4-Dihydroxycyclo-2,5-diene Precursors. *Chem. Eur. J.* **2015**, 21, 5742–5749.
- (26) Iwamoto, T.; Watanabe, Y.; Sakamoto, Y.; Suzuki, T.; Yamago, S. Selective and Random Syntheses of [n]Cycloparaphenylenes (n = 8–13) and Size Dependence of Their Electronic Properties. *J. Am. Chem. Soc.* **2011**, *133*, 8354–8361.
- (27) Xia, J.; Jasti, R. Synthesis, Characterization, and Crystal Structure of [6] Cycloparaphenylene. *Angew. Chem., Int. Ed.* **2012**, *51*, 2474–2476.
- (28) Frisch, M. J.; et al. Gaussian 16, Gaussian, Inc.: Wallingford, CT, 2016.
- (29) Ernzerhof, M.; Scuseria, G. E. Assessment of the Perdew–Burke–Ernzerhof exchange-correlation functional. *J. Chem. Phys.* **1999**, *110*, 5029–5036.
- (30) Patel, G. N.; Chance, R. R.; Witt, J. D. A planar—nonplanar conformational transition in conjugated polymer solutions. *J. Chem. Phys.* **1979**, *70*, 4387–4392.
- (31) Cui, C. X.; Kertesz, M.; Jiang, Y. Extraction of polymer properties from oligomer calculations. *J. Phys. Chem.* **1990**, 94, 5172–5179.
- (32) Nishihara, T.; Segawa, Y.; Itami, K.; Kanemitsu, Y. Excited States in Cycloparaphenylenes: Dependence of Optical Properties on Ring Length. *J. Phys. Chem. Lett.* **2012**, *3*, 3125–3128.
- (33) Adamska, L.; Nayyar, I.; Chen, H.; Swan, A. K.; Oldani, N.; Fernandez-Alberti, S.; Golder, M. R.; Jasti, R.; Doorn, S. K.; Tretiak, S. Self-Trapping of Excitons, Violation of Condon Approximation, and Efficient Fluorescence in Conjugated Cycloparaphenylenes. *Nano Lett.* **2014**, *14*, 6539–6546.
- (34) During the review and revision process for this manuscript, Pingwu Du and co-workers published a communication in this journal reporting a CPP-based conjugated polymer conceptually carved out of a prototypical carbon nanotube: A Long Pi-Conjugated Poly(para-Phenylene)-Based Polymeric Segment of Single-Walled Carbon Nanotubes. J. Am. Chem. Soc. 2019, 141, 18938—18943.